Proceedings of the 20th International Conference on Soil Mechanics and Geotechnical Engineering– Rahman and Jaksa (Eds)

Electrical resistivity characteristics of rock fractures according to aperture size

Caractéristiques de résistivité électrique de la fracture de la roche en fonction de la taille de l'ouverture

Tae-Hyun Kong, Tae-Min Oh, Jong-Won Lee
Department of Civil and Environmental Engineering, Pusan National University, Republic of Korea, elffk94@gmail.com

Hang-bok Lee
Korea Institute of Geoscience and Mineral Resources, Republic of Korea

ABSTRACT: Underground structures (e.g., storage for CO_2) have been used to minimize risks such as climate change. During the utilization of such structures, CO_2 can leak through rock fractures in the underground rock medium caused by unexpected damage or natural weathering. Therefore, it is important to investigate rock fracture characteristics such as aperture size to ensure the safe application of underground structures. The electrical resistivity technique is a useful method of identifying characteristics of rock fractures and one that is often utilized for long-term monitoring. In this study, the electrical resistivity test was performed to evaluate the effects of rock aperture size in rock fractures under underground water conditions. Artificial rock fractures were prepared according to aperture size (4─15 mm) and pore fluid resistivity (0.2─180 Ω·m). In addition, the frequency range and circuit mode (e.g., series or parallel) were selected to obtain more reliable measurements. According to the test results, electrical resistivity exponentially decreases as aperture size increases. This study is expected to provide a basic foundation for electrical resistivity monitoring of underground rock structures.

KEYWORDS: Electrical resistivity; Rock fracture; Aperture size; Monitoring; Formation factor

1 INTRODUCTION

Rocks are ideal as cap rocks for sealing CO_2 storage structures due to their impermeable properties. However, rocks can be fractured by unexpected damage (e.g., earthquakes) or natural weathering. For underground structure applications such as CO_2 storage, it is important to analyze the characteristics of rock fractures (e.g., aperture size and shape) as this can cause the stored CO_2 to leak with groundwater. The electrical resistivity technique has been proposed as a useful method of evaluating rock fracture characteristics such as an aperture size and degree of weathering (Nakatsuka et al., 2010; Oh et al., 2015).

1.1 *Background of formation factor*

Under fully saturated conditions, the formation factor (F) is determined by the following electrical resistivity of rock-pore fluid resistivity correlation equation given by Equation (1) (Archie, 1947).

$$F = \rho_{bulk}/\rho_f \quad (1)$$

Where ρ_{bulk} is bulk electrical resistivity and ρ_f is pore fluid resistivity. The formation factor is a function of rock properties such as cementation factor, pore geometry, and tortuosity under constant pore fluid resistivity. Thus, the formation factor is strongly related to the permeability of a rock medium.

1.2 *Research purpose*

In this study, bulk resistivity and pore fluid resistivity for single rock fractures are measured according to aperture size to obtain the formation factor. Aperture size is considered in the range of 4─15 mm with various pore fluid resistivities (0.2─180 Ω·m).

2 EXPERIMENTAL PROGRAM

2.1 *Specimen and test cell*

Artificial rock specimens (150 mm in length, 40 mm in width, and 120 mm in height) were prepared with acetal materials to reproduce varying degrees of roughness, which affects the electrical resistivity of rocks. The test cell (150 mm in length, 100 mm in width, and 100 mm in height) was made of transparent polyvinyl chloride (PVC) material. Stainless steel electrodes (5 mm in diameter and 12.5 mm in length of gap) were installed in the lateral walls to measure the electrical resistance.

2.2 *Electrical measurement system*

The test system consisted of an LCR meter (Keysight, E4980A), a DAQ system (Keysight, 34972A), and data storage (Fig. 1). The electrical resistance of each specimen was measured using the LCR meter, which was able to measure in the frequency range of 0 Hz─2 MHz and a voltage range of 0.1─20 V.

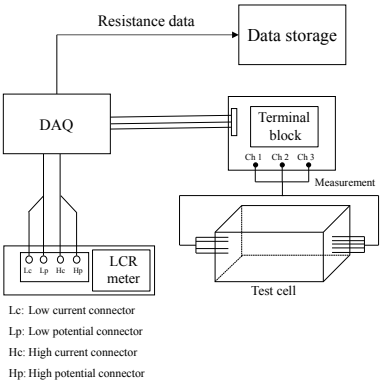

Figure 1. Multichannel electrical resistivity measurement system with high current (H_c), high potential (H_p), low current (L_c), and low potential (L_p)

The cores of the high current (H_c) and high potential (H_p) were soldered and connected to one electrode, whereas the cores of the low current (L_c) and low potential (L_p) were soldered and connected to the other electrode. During the experiment, the current flowed from H_c to L_c, and the resistance was measured using the two potential electrodes (H_p and L_p). The DAQ system was compatible with the LCR meter for collecting multichannel data. The data storage was used to store the resistance readings. Three channels and three pairs of electrodes were prepared to obtain multiple electrical resistance measurements. The mean value of ten resistance measurements was obtained for each experimental case. In terms of the type of current used, as direct current (DC) electrical fields can cause charged ions to migrate in porous media, resulting in electro-osmosis, alternating current (AC) was used to measure electrical resistance; this is due to the potential effects of electro-osmosis on soil properties.

2.3 *Experimental procedures*

Pairs of artificial rock specimens were mounted inside the test cell, and the aperture (the void space between the pair of specimens) was completely saturated with pore fluid. The electrical resistance of each specimen was measured for various aperture sizes (4–15 mm) and pore fluid resistivities (0.2–180 Ω·m).

Electrical resistance was measured at least ten times to provide an average value. After the experiment, the pore fluid resistivity in the test cell was measured with an electrical conductivity meter (XEBEX, CM-30R). All test procedures for measuring electrical resistivity were conducted under a constant temperature of 19 ± 1.5 ℃ due to the potential effects of temperature on electrical resistivity.

3 DETERMINATION OF FREQUENCY AND CIRCUIT

The operating frequency range was determined by conducting frequency sweeping with consideration of electrical resonance in the circuit. Frequency sweeps (20 Hz–1 MHz) were performed to determine the optimal frequency for solid resistance (47 Ω–100 kΩ) and fluid resistance (1.04 Ω·m–100 Ω·m).

3.1 *Solid resistance*

Fig. 2 and Fig. 3 show resistance data obtained for various levels of solid resistance. 47 Ω to 1 kΩ is defined as low resistance, whereas 4.7 kΩ to 1 MΩ is defined as high resistance.

Fig. 2 shows the resistance data obtained for various levels of solid resistance using the series circuit mode. Fig. 2(a) shows the logarithmical values of resistance as a function of logarithmic frequency for various low resistances, and Fig. 2(b) shows the same results but for high resistances. Electronic resonance occurred for low resistances at frequencies higher than 50 kHz and for high resistances at frequencies higher than 2 kHz. The results indicate that materials with high resistance, like granite, exhibit stable resistance responses below 2 kHz.

Fig. 3 shows the resistance data obtained for various levels of solid resistance using the parallel circuit mode. Fig. 3(a) shows the logarithmical value of resistance as a function of frequency in the logarithmic scale for low resistances, and Fig. 3(b) shows the same results but for high resistances. Electronic resonance occurred for low resistances at frequencies higher than 90 kHz and for high resistances at frequencies higher than 50 kHz. The results show that the resistance values are stable at frequencies below 50 kHz.

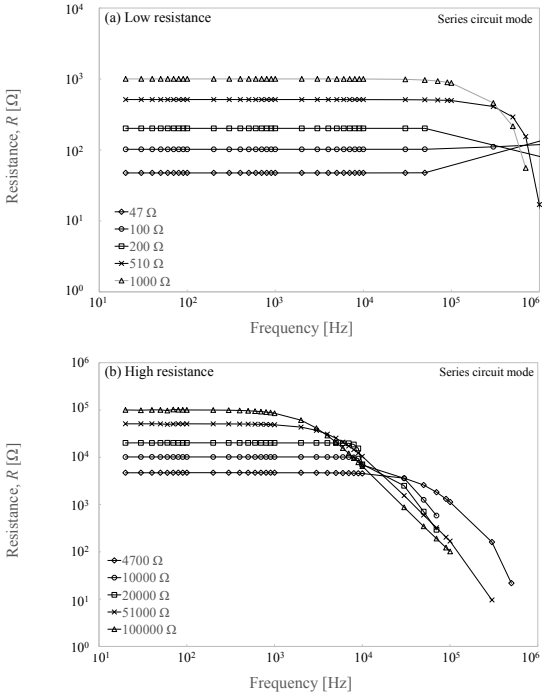

Figure 2. Resistance versus frequency measured for resistors of varying resistances (voltage = 1V) using the series circuit mode: (a) low resistance (47–1000 Ω) and (b) high resistance (4.7–1000 kΩ)

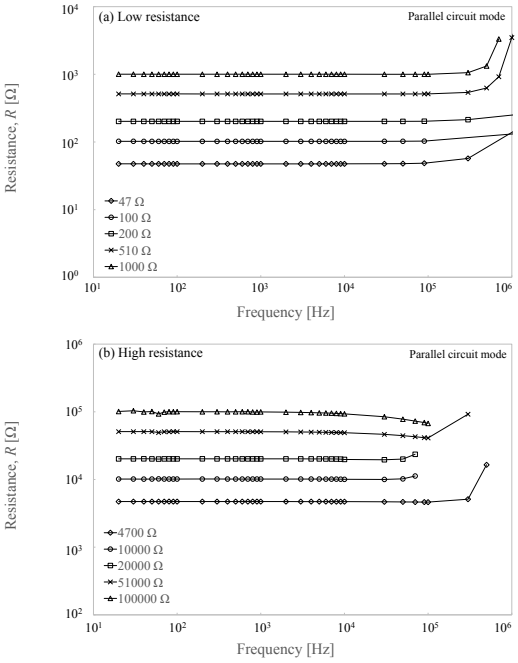

Figure 3. Resistance versus frequency measured for resistors of varying resistances (voltage = 1V) using the parallel circuit mode: (a) low resistance (47–1000 Ω) and (b) high resistance (4.7–1000 kΩ)

3.2 *Fluid resistance*

Fig. 4 shows the electrical resistances of ionic NaCl solutions with varying electrical resistivities (1.04 Ω·m, 5.29 Ω·m, 10.2 Ω·m, 50 Ω·m, and 100 Ω·m) in the frequency range of 20 Hz to 1 MHz for the series circuit mode.

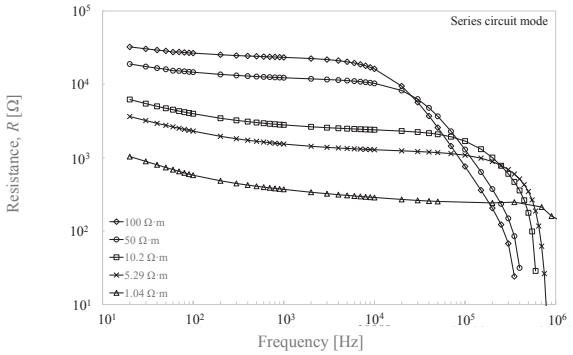

Figure 4. Electrical resistances of various NaCl concentrations (1.04─100 Ω·m) in the frequency range of 20 Hz to 2 MHz for the series circuit mode

The electrical resistance of the NaCl solution with 5.29 Ω·m resistivity decreased up to a frequency of 350 kHz; beyond this point, resistance significantly decreases with increasing frequency. In addition, the electrical resistance of the NaCl solution with a resistivity of 100 Ω·m slightly decreased up to a frequency of 9 kHz; beyond this point, the resistance also significantly decreases with increasing frequency. As the electrical resistivity of the NaCl solution increases, electronic resonance occurs at lower frequencies (e.g., 10 kHz). On the other hand, for the parallel circuit mode, the electrical resistance of NaCl solution decreases up to a resonance frequency (e.g., 250 kHz), after which the resistance significantly increases with increasing frequency.

According to the frequency sweeping results, resistance can be reliably measured between 700 Hz and 9 kHz using the series circuit mode and between 1 kHz and 250 kHz using the parallel circuit mode. It is noteworthy that the parallel circuit mode exhibits a wider stable frequency range than the series circuit mode.

4 CELL CALIBRATION

Electrical resistance (R) is affected by several factors, such as the shape of the cell, cable length, and the type of electrode material. Therefore, a calibration process is essential to convert electrical resistance into electrical resistivity (ρ), which is indicated by inherent electrical characteristics. Electrical resistivity is determined by Equation (2).

$$\rho = \alpha \cdot R \tag{2}$$

α is a shape factor that can be determined through a calibration test. For the calibration, electrical resistance was measured using the LCR meter and electrical resistivity was subsequently measured using the electrical conductivity meter. This process was repeated with the addition of sodium chloride (NaCl) to water, which increases the ionic concentration. Electrical resistance and electrical resistivity were then measured according to the concentration of NaCl. The calibration test results are shown in Fig. 5. The shape factor was obtained as 0.0049 m for the series circuit mode and 0.0043 m for the parallel circuit mode under the measurement conditions of 1 V and 1 kHz.

5 RESULTS

5.1 *Effects of pore fluid resistivity*

The electrical properties of fully saturated rocks are governed by pore fluid resistivity in rock fractures. In the field, electrical resistivity values are generally obtained in the range of 20–200 Ω·m in groundwater and less than 0.5 Ω·m in seawater (Park, 2004; Saad et al, 2012). Fig. 6 shows the results of formation factor according to pore fluid resistivity (P1 = 176.6 Ω·m, P2 = 25.2 Ω·m, and P3 = 0.239 Ω·m) for two aperture sizes (5 and 15 mm).

Fig. 6(a) shows the formation factor results according to pore fluid resistivity for each circuit mode with an aperture size of 5 mm. The value of P2 is 1.1 times greater than P1, and the value of P3 is 4.7 times greater value than P1 in the parallel circuit mode. In the series circuit mode, the value of P2 is 1.3 times greater than P1, and the value of P3 is 3.8 times greater than P1.

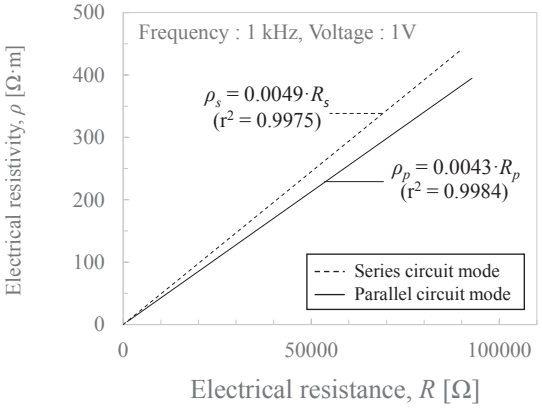

Figure 5. Electrical resistivity calibration of the test cell

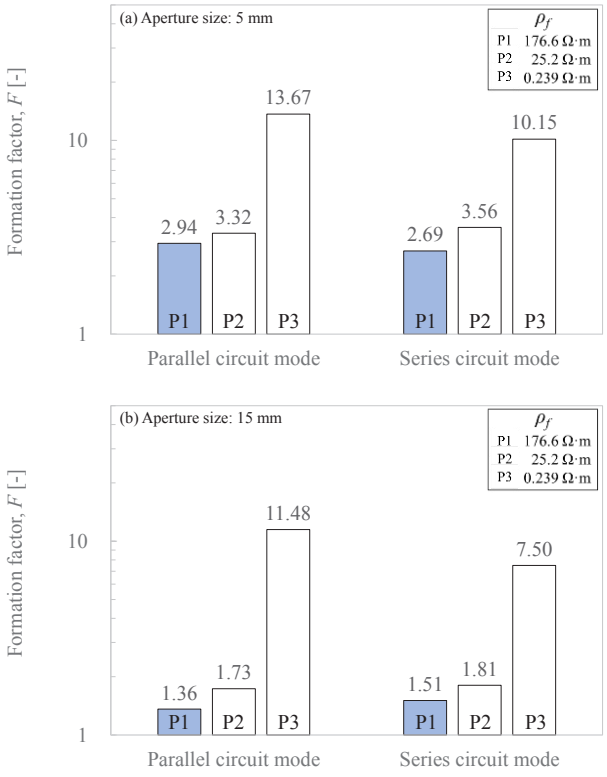

Figure 6. Relationship between the formation factor and pore fluid resistivity with a fixed aperture size: (a) 5 mm and (b) 15 mm

Fig. 6(b) shows the formation factor results according to pore fluid resistivity for each circuit mode with an aperture size of 15 mm. The value of P2 is 1.3 times greater than P1, and the value of P3 is 8.4 times greater than P1 in the parallel circuit mode. In the series circuit mode, the value of P2 is 1.2 times greater than P1, and the value of P3 is 5.0 times greater than P1.

The results indicate that the formation factor exhibits

remarkable variation according to the decrease in pore fluid resistivity from groundwater to seawater conditions. Compared to the rock specimens with the small aperture size, the increase in formation factor according to pore fluid resistivity was greater for the rock specimens with the large aperture size.

5.2 *Effects of aperture size*

Fig. 7 shows the change in the formation factor according to aperture size (4–15 mm) under various pore fluid resistivity conditions.

Fig. 7(a) and Fig. 7(b) show the results of the electrical resistivity test under groundwater conditions. As aperture size is increased from 4.0 mm to 15.0 mm, the formation factor decreases from 3.5 to 1.6. On the other hand, Fig. 7(c) shows the results of the electrical resistivity test under seawater conditions. In this case, as aperture size is increased from 4.0 mm to 15.0 mm, the formation factor decreases from 12.6 to 9.5.

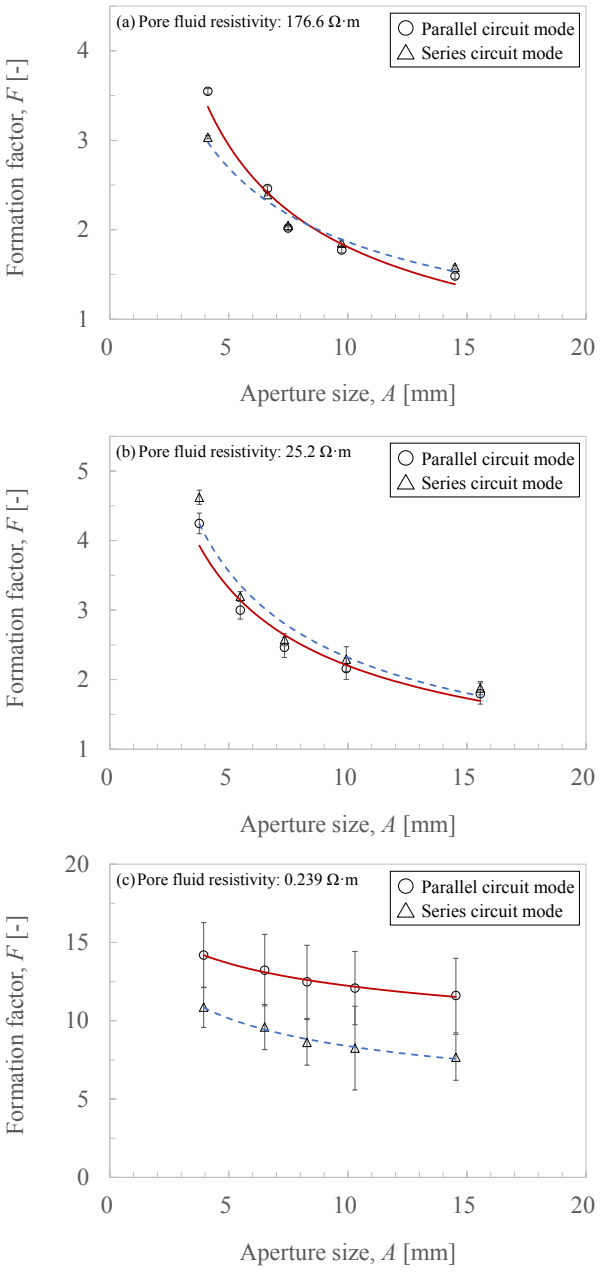

Figure 7. Formation factor according to aperture size under various pore fluid resistivities: (a) 176.6 Ω·m, (b) 25.2 Ω·m, and (c) 0.239 Ω·m

According to the results, the formation factor exponentially decreases as the aperture size increases under groundwater conditions, whereas the formation factor slightly decreases upon increasing aperture size under seawater conditions. The results indicate that the formation factor is more sensitive to aperture size changes under groundwater conditions than seawater conditions. The lower sensitivity of the formation factor under seawater conditions is due to ion diffusion caused by the higher ion concentration (Choo et al., 2011).

6 CONCLUSIONS

In this study, the formation factor was evaluated according to electrical resistivity and aperture size. An experimental study was conducted using artificial rock specimens with various aperture sizes and pore fluid resistivity values.

The results demonstrated that the formation factor exhibits remarkable variation according to the pore fluid characteristics. Compared to specimens with a smaller aperture size, the formation factor exhibited a greater increase according to pore fluid resistivity in specimens with a larger aperture size.

On the other hand, the formation factor exponentially decreases as aperture size increases under groundwater conditions, whereas under seawater conditions, the formation factor slightly decreases as aperture size increases. Therefore, it can be concluded that the formation factor is more sensitive to aperture size changes under groundwater conditions compared to seawater conditions.

In underground rock media, fluid behavior is dependent on the hydraulic properties (i.e., permeability) of rock fractures. Permeability, which is dominantly determined by aperture size, is highly correlated to the formation factor of resistivity. Thus, the electrical resistivity technique can be applied to rock fractures under underground water conditions to estimate aperture size and monitor permeability. This study is expected to provide a basic foundation for electrical resistivity monitoring of rock fractures around underground rock structures.

7 ACKNOWLEDGEMENTS

This research was supported by the National Research Foundation of Korea (NRF) grant funded by the Korea Government (MSIT) (No. NRF-2019R1G1A1100517) and by the Brain Korea 21 FOUR Project in the Education & Research Center for Infrastructure of Smart Ocean City (i-SOC Center).

8 REFERENCES

Archie, G. E. 1947. Electrical resistivity an aid in core-analysis interpretation. AAPG Bulletin, 31(2), 350-366.

Choo, M. K., Song, I. S., Lee, H. K., Kim, T. H., & Chang, C. D. 2011. Application of the electrical impedance of rocks in characterizing pore geometry. The Journal of Engineering Geology, 21(4), 323-336.

Nakatsuka, Y., Xue, Z., Garcia, H., Matsuoka, T. 2010. Experimental study on CO2 monitoring and quantification of stored CO2 in saline formations using resistivity measurements, International Journal of Greenhouse Gas Control, 4(2), 209-216.

Oh, T. M., Cho, G. C., Son, T. A., Ryu, H. H., Lee, C. 2015. Experimental approach to evaluate weathering condition of granite using electrical resistivity. Geomechanics and Engineering, 8(5), 675-685.

Park, S. G. 2004. Physical property factors controlling the electrical resistivity of subsurface. Geophysics and Geophysical Exploration, 7(2), 130-135.

Saad, R., Nawawi M. N. M, Mohamad E. T. 2012. Groundwater Detection in Alluvium Using 2- D Electrical Resistivity Tomography (ERT). Electronic Journal of Geotechnical Engineering. 17, 369-376